

Supporting Information

Benign electrolytic modifications of starch: Effects on functional groups and physical properties

Pitcha Liewchirakorn,^{1,2} Kamonwad Ngamchuea^{1,*}

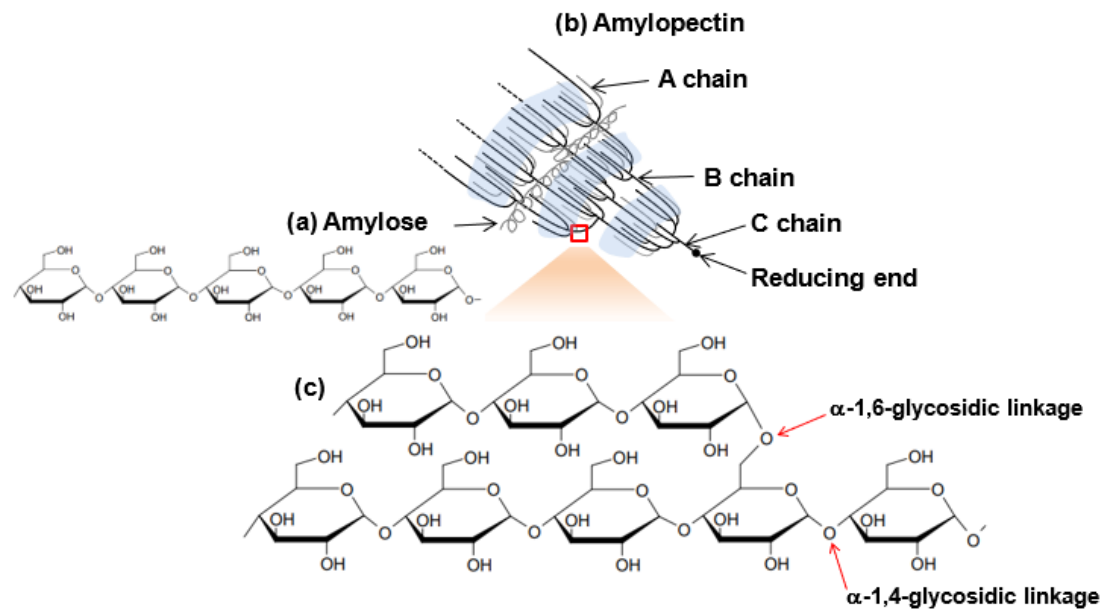
¹ School of Chemistry, Institute of Science, Suranaree University of Technology, 111 University Avenue, Suranaree, Muang, Nakhon Ratchasima 30000, Thailand

² Institute of Research and Development, Suranaree University of Technology, 111 University Avenue, Suranaree, Muang, Nakhon Ratchasima, 30000, Thailand

*Corresponding author: Kamonwad Ngamchuea, School of Chemistry, Institute of Science, Suranaree University of Technology, 111 University Avenue, Suranaree, Muang, Nakhon Ratchasima, 30000, Thailand. Email: kamonwad@g.sut.ac.th; Tel: +66 (0) 44 224 637

S1 Typical structure of cassava starch granules

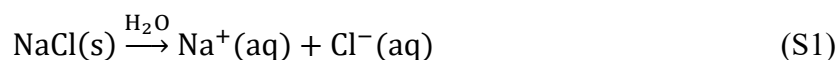
Scheme S1 below illustrates the typical structure of cassava starch granules.



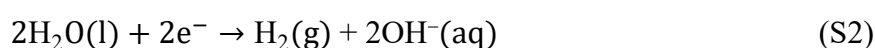
Scheme S1: Schematic diagram presenting the structures of (a) amylose, (b) amylopectin with the typical arrangement in the starch granule, and (c) α -1,4- and α -1,6- glycosidic linkages in amylopectin.

S2 Electrochemical reactions during electrolysis

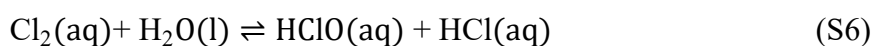
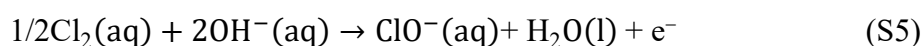
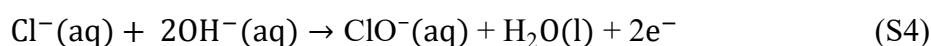
Sodium chloride (NaCl) dissolves in water and dissociates to form Na⁺ and Cl⁻ (eqn. S1). During electrolysis, an electric voltage is applied between electrodes, causing oxidation and reduction reactions to take place at the anode and cathode, respectively. At the cathode, H₂O molecules undergo a reduction reaction, generating hydrogen gas (H₂) and hydroxide ions (OH⁻), refer to eqn. S2. At the anode, the oxidation of Cl⁻ occurs, resulting in the formation of chlorine gas (Cl₂), which can dissolve in the solution (eqn. S3). The OH⁻ (generated at the cathode) can then further react with Cl⁻ (in the bulk solution, eqn. S4) and Cl₂ (generated at the anode, eqn. S5), leading to the formation of the hypochlorite ion (ClO⁻). The generated Cl₂ can also enhance the formation of hydrochloric acid (HCl) and hypochlorous acid (HClO) via the reaction with water, refer to eqn. S6. The main chemical reactions that occur in the electrolysis cell are summarized as follows ¹:



Cathode:



Anode:



The predominant chlorine species within the electrolytic cell are dictated by the compositions of Cl_2 , HClO , and ClO^- at different pH levels. This relationship is depicted in Figure S1.^{1,2}

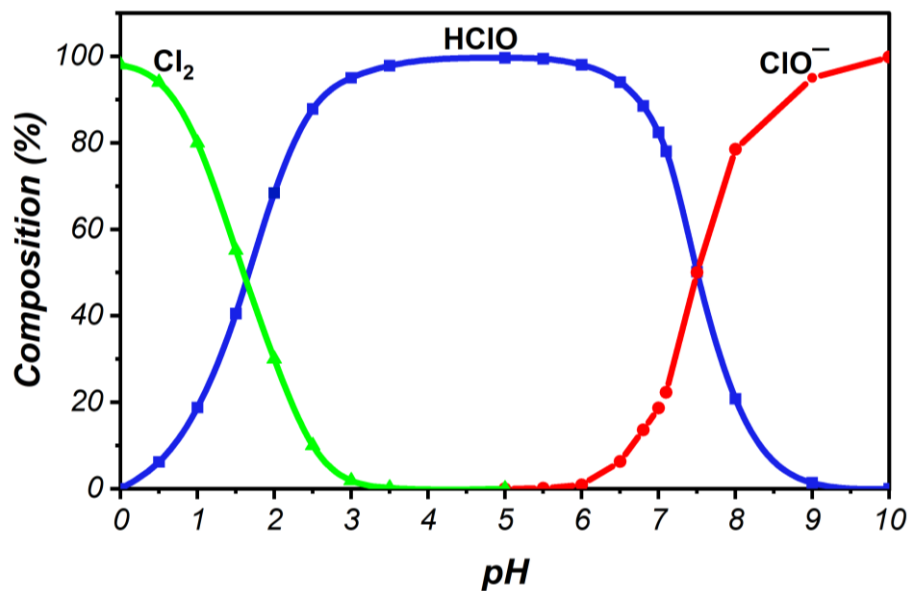


Figure S1: Speciation of aqueous chlorine species (Cl_2 , HClO , ClO^-) as a function of pH.

S3 Electrode characterization before and after electrolysis

The surface of the electrodes was imaged before and after electrolysis using an optical microscope (Axiocam 105 color, ZEISS, Germany) at 5x magnification. No significant change in the electrode surface was observed, refer to Figure S2.

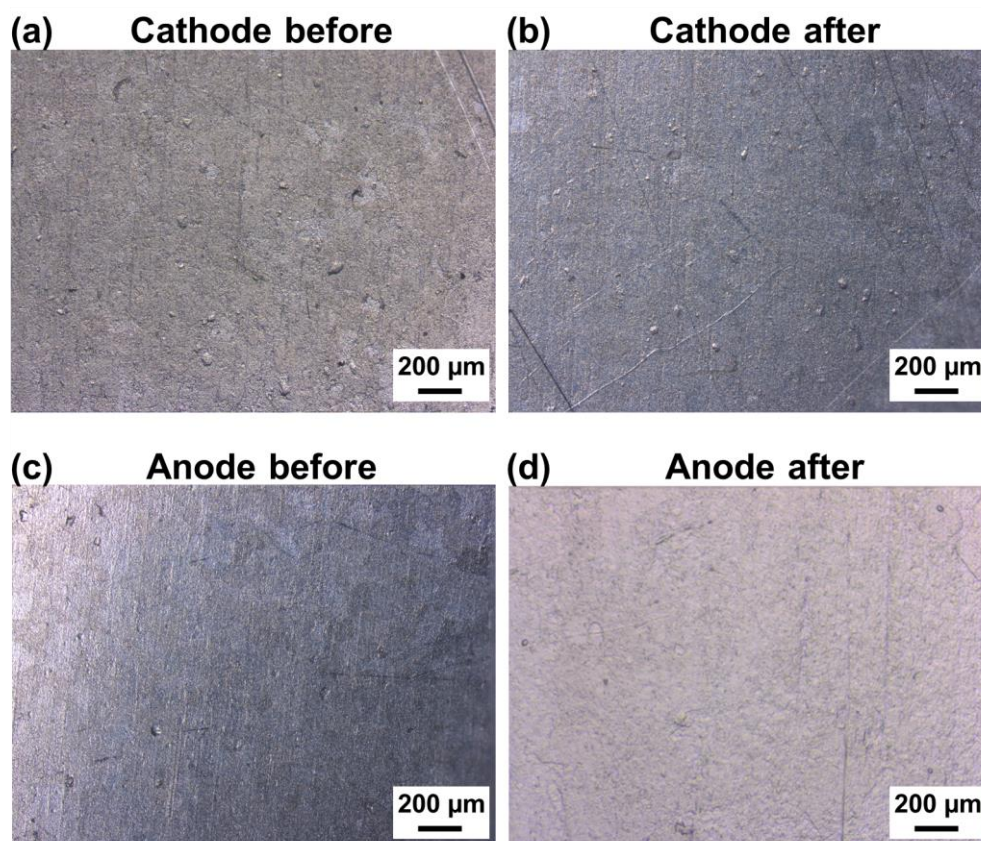


Figure S2: Microscopic images of cathode and anode before and after electrolysis of starch in 15 wt% NaCl at 24 V for 30 minutes.

The electroactivity of the electrodes before and after electrolysis was assessed using a standard redox probe, $[\text{Fe}(\text{CN})_6]^{4-/3-}$, at a scan rate of 50 mV s^{-1} . The results in Figure S3 demonstrate that the activity of both the cathode and anode decreased after electrolysis, possibly due to some degree of electrode passivation during the electrolysis process. However, the electroactivity of the electrodes can be restored after electrode cleaning, which was achieved by immersing the electrodes in a 0.10 M HCl solution for 2 minutes. This was followed by

mechanical polishing using alumina slurry (1.0, 0.3, and 0.05 μm , Buehler, USA) on soft polishing microcloths (Buehler, USA) and subsequent sonication to remove any remaining alumina on the surface.

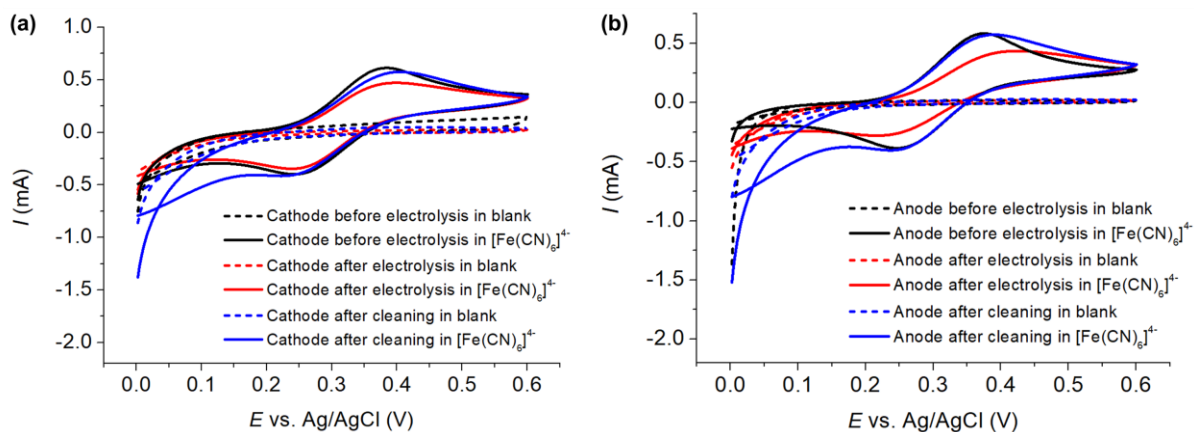


Figure S3: Cyclic voltammetry of 1.0 mM $[\text{Fe}(\text{CN})_6]^{4-}$ in 0.10 M KCl at a scan rate of 50 mV s^{-1} for the cathode and anode before and after electrolysis of starch in a 15 wt% NaCl solution at 24 V for 30 minutes.

S4 Pasting properties of native and oxidized starches

Table S1 below presents the pasting properties of native and oxidized starches measured using the Rapid Visco-Analyzer.

Table S1: Pasting properties of native and oxidized starches

Samples	Electrolysis conditions	PT (°C)	PV (cP)	TV (cP)	BVD (cP)	FV (cP)	SBV (cP)
Native starch	-	68.3±0.1	1,996±62.2	931.3±22.5	1064.7±39.7	1,511.0±24.0	579.7±1.6
Oxidized starch	5 wt% NaCl, 12V, 30 min	69.1±0.0	1,462.5±44.5	456.8±11.7	1005.7±32.8	869.4±32.0	412.6±20.3
	5 wt% NaCl, 24V, 30 min	71.4±0.3	981.1±20.4	106.0±1.1	875.1±21.5	134.5±6.9	28.5±5.8
	15 wt% NaCl, 12V, 30 min	70.4±0.0	752.2±46.0	N/A	N/A	90.3±1.1	N/A
	10 wt% NaCl, 12V, 120 min	73.5±0.4	285.2±7.5	N/A	N/A	81.4±0.2	N/A
	15 wt% NaCl, 24V, 30 min	72.3±0.1	153.5±1.2	N/A	N/A	73.0±1.8	N/A
	15 wt% NaCl, 24V, 120 min	N/A	N/A	N/A	N/A	91.0±1.2	N/A

PT: pasting temperature, PV: peak viscosity, TV: trough viscosity, BVD: breakdown viscosity, FV: final viscosity, SBV: set back viscosity, N/A: not available.

References

1. Ronco, C.; Mishkin, G. J., *Disinfection by sodium hypochlorite: dialysis applications*. Karger Medical and Scientific Publishers: 2007; Vol. 154.
2. Hung, Y.-C.; Waters, B. W.; Yemmireddy, V. K.; Huang, C.-H., pH effect on the formation of THM and HAA disinfection byproducts and potential control strategies for food processing. *Journal of Integrative Agriculture* **2017**, *16* (12), 2914-2923.
3. Vanier, N. L.; El Halal, S. L. M.; Dias, A. R. G.; da Rosa Zavareze, E., Molecular structure, functionality and applications of oxidized starches: A review. *Food Chemistry* **2017**, *221*, 1546-1559.
4. Dimri, S.; Aditi; Bist, Y.; Singh, S., Oxidation of Starch. In *Starch: Advances in Modifications, Technologies and Applications*, Sharanagat, V. S.; Saxena, D. C.; Kumar, K.; Kumar, Y., Eds. Springer International Publishing: Cham, 2023; pp 55-82.